Journal of Applied Ecology

Bachofen Christoph (Orcid ID: 0000-0002-5269-0299)
Poyatos Rafael (Orcid ID: 0000-0003-0521-2523)
Grossiord Charlotte (Orcid ID: 0000-0002-9113-3671)

Stand structure of Central European forests matters more than climate for transpiration sensitivity to VPD

Christoph Bachofen[1,2], Rafael Poyatos[3,4], Víctor Flo[4,5], Jordi Martínez-Vilalta[3,4], Maurizio Mencuccini[3,6], Víctor Granda[3], Charlotte Grossiord[1,2]

[1] Plant Ecology Research Laboratory PERL, School of Architecture, Civil and Environmental Engineering, EPFL, Lausanne CH-1015, Switzerland

[2] Functional Plant Ecology, Community Ecology Unit, Swiss Federal Institute for Forest, Snow and Landscape WSL, Lausanne CH-1015, Switzerland

[3] CREAF, Bellaterra (Cerdanyola del Vallès), Catalonia, E08193 Spain

[4] Universitat Autònoma de Barcelona, Bellaterra (Cerdanyola del Vallès), Catalonia, E08193 Spain

[5] Imperial College London, Department of Life Sciences, Silwood Park Campus, Ascot SL5 7PY, UK

[6] ICREA, Pg. Lluís Companys 23, Barcelona, 08010, Spain

Abstract

1. Temperature rise and more severe and frequent droughts will alter forest transpiration, thereby affecting the global water cycle. Yet, tree responses to increased atmospheric vapour pressure deficit (VPD) and reduced soil water content (SWC) are not fully understood due to long-term tree adjustments to local environmental conditions that modify transpiration responses to short-term VPD and SWC changes.
2. We analysed sap flux density (SFD) of *Fagus sylvatica*, *Picea abies*, *Pinus sylvestris,* and *Quercus ilex* from 25 sites across Europe to understand how daily variation in SWC affects the sensitivity of SFD to VPD (β_{VPD}) and the maximum SFD (S_{95}). Furthermore, we tested whether long-term adjustments to site climatic conditions and stand characteristics affect β_{VPD} and S_{95}.
3. The studied species showed contrasting β_{VPD} and S_{95} with the largest values in *F. sylvatica*, followed by *Q. ilex*, which surpassed the two conifers that showed low β_{VPD} and low S_{95}. We observed that β_{VPD} and S_{95} dropped during days of low SWC in *F. sylvatica*, *P. sylvestris,* and *Q. ilex*, but not in *P. abies*. Both β_{VPD} and S_{95} were driven by tree height, and the temperature and precipitation at the sites. However, stand basal area was the most important driver of β_{VPD} and S_{95}, explaining 30% of their total variance.
4. *Synthesis and applications:* A future warmer and drier climate will restrict tree transpiration and thereby heavily affect the soil-plant-atmosphere coupling. However, the effect of basal area, being the largest driver of tree transpiration sensitivity to vapour pressure deficit across a broad range of conditions, provides the opportunity to pre-adapt European forests to future climate conditions. While stand thinning can increase the soil water availability for remaining trees, it also increases transpiration sensitivity to high air temperatures and may thereby amplify tree vulnerability to heat and drought.

Keywords: Basal area, Fagus sylvatica, Picea abies, Pinus sylvestris, Quercus ilex, sap flow, SAPFLUXNET, vapour pressure deficit

Introduction

Forests transpire more than 50% of terrestrial precipitation and thus constitute a key component of the global water cycle (Schlesinger & Jasechko, 2014; Stoy et al., 2019). Air temperatures have recently increased globally, while relative humidity has remained constant (Dai, 2006; McCarthy et al., 2009). As a consequence, the vapour pressure deficit (VPD) of the atmosphere has increased globally (e.g., Ficklin & Novick, 2017), which might lead to higher forest transpiration (Granda et al., 2020; Grossiord et al., 2020). At the same time, changes in precipitation patterns, including more frequent droughts, may limit forest transpiration (Grossiord et al., 2019; Liu et al., 2020) and increase the risk of drought-induced forest decline (McDowell et al., 2022). To anticipate future changes in the global water cycle and forest drought responses, we need to better understand the combined effect of higher air temperatures and decreased soil water availability on forest transpiration.

Rising VPD affects tree transpiration in two ways: first, it comes with an increase in the evaporative demand and thus a higher force driving the water loss through stomata, and second, it induces stomatal closure through its effect on leaf water status (Cochard et al., 2002; Monteith, 1995). Therefore, transpiration responses to changes in VPD take a non-linear shape, with an initial increase until a certain threshold where the maximum is reached, after which stomatal closure may result in decreased transpiration (Monteith, 1995). Transpiration regulation in response to changes in VPD is highly species-specific due to differences in hydraulic architecture (Flo et al., 2021; Grossiord et al., 2017; Hassler et al., 2018; Peters et al., 2019). Climate change impacts plants not only through changes in VPD but also soil drought, leading to shifts in the balance between the demand and supply for water (evapotranspiration *vs*. precipitation; Novick et al., 2016). Drought-stressed trees respond to soil moisture deficit by inducing stomatal closure (Running, 1976), resulting in the reduction of both transpiration and photosynthesis (e.g.: Martínez-Vilalta & Garcia-Forner, 2017; Mencuccini et al., 2015).

The sensitivity of stomatal responses to changes in soil water availability largely depends on the plant stomatal behaviour, which ranges along a continuum from isohydric to anisohydric strategy across species (Klein, 2014; Martínez-Vilalta et al., 2014; Martínez-Vilalta & Garcia-Forner, 2017). Soil water availability and VPD thus co-determine stomatal conductance through their mutual effect on the leaf water potential.

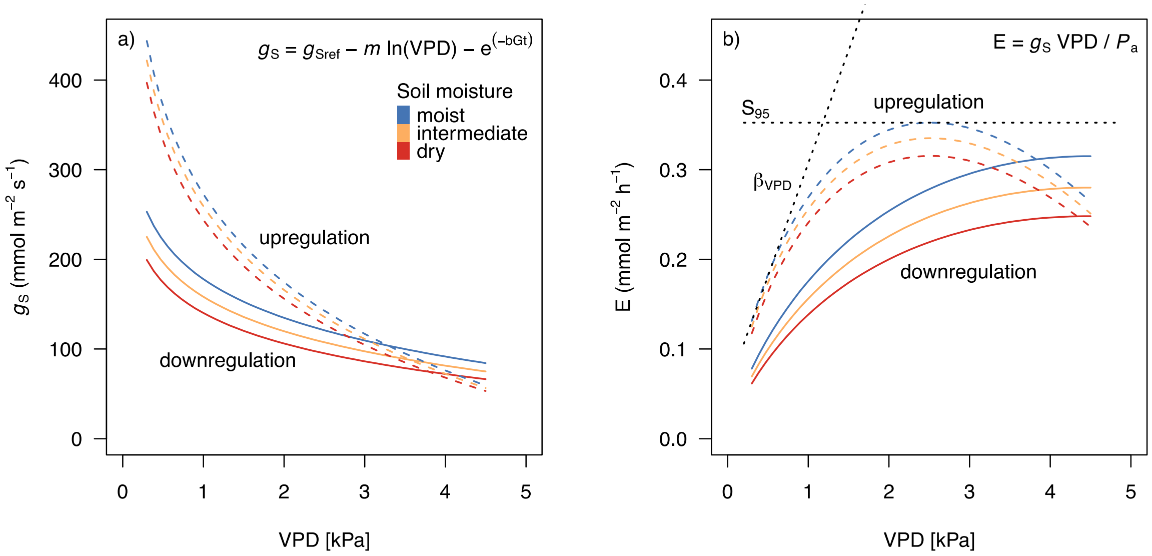

Fig. 1: Schematic representation of (a) Stomatal conductance (g_S) and (b) transpiration (E) in relation to VPD at different soil moisture (moist, intermediate, dry). Populations may adjust to long-term environmental conditions by downregulating (solid lines) the transpiration sensitivity to VPD (β_{VPD}) and maximum transpiration (S_{95}) whereas other populations under different long-term environmental conditions may upregulate them (dashed lines). g_S is regulated by the maximum g_S (g_{Sref}) at low VPD, the stomatal sensitivity to VPD (m), the hydraulic conductance of the soil-to-leaf pathway (Gt), and the stomatal sensitivity to Gt (b) (Meinzer, 2003). E is driven by g_S, the VPD, and the air pressure (P_a) (Oren et al., 1999).

While we have a relatively good understanding of the mechanisms of short-term transpiration responses to changes in VPD and soil moisture at the leaf and tree levels, our knowledge of intraspecific variability of transpiration regulation along environmental gradients is minimal.

Some studies observed higher sap flow sensitivity to VPD across species in dry compared to moist sites (e.g. Denham et al., 2021). Moreover, within-species comparisons showed higher sap flow rates and higher sap flow sensitivity to VPD in warmer and soil-drought exposed populations of a species (Maherali & DeLucia, 2001; Poyatos et al., 2007). Such observations of intraspecific variability are consistent with studies showing higher stomatal conductance at high VPD of warm acclimated seedlings (Marchin et al., 2016), which indicates prioritisation of carbon uptake and thermal leaf regulation at the risk of higher transpirational water loss ('upregulation' scenario, Fig. 1). However, other studies have reported decreased canopy conductance and lower stomatal sensitivity to VPD under long-term high VPD conditions (Grossiord et al., 2017), indicating long-term downregulation of tree transpiration to maintain hydraulic functioning ('downregulation' scenario, Fig. 1).

In addition to adjustments to climatic conditions, soil hydrodynamic properties and stand structure can modulate the physiological responses among populations of a species. Sandy soils have been associated with higher canopy conductance and increased stomatal sensitivity to VPD in *Pinus palustris* compared to loamy soils (Addington et al., 2006). Furthermore, trees in less dense stands tend to have higher transpiration rates per unit sapwood area (Caballé et al., 2016), as typically observed after stand thinning (Gebhardt et al., 2014). However, we do not know how transpiration sensitivity to VPD varies with stand structure and whether these physiological adjustments are related to tree-level water transport properties (Whitehead et al., 1984) for different species, as already observed across *Pinus sylvestris* populations (Poyatos et al., 2007).

We investigated how climate, soil properties, and stand characteristics modulate the transpiration sensitivity of trees to VPD and soil water availability by analysing sap flux data on a continental scale. Using the SAPFLUXNET database, we investigated four important

European tree species with contrasting water-use strategies, *Fagus sylvatica*, *Picea abies*, *Pinus sylvestris,* and *Quercus ilex*, from multiple sites along climatic gradients. We related maximum sap flux density (S_{95}) and sap flux sensitivity to VPD (β_{VPD}) to each site's soil, climate, and stand characteristics. We expected that (1) low soil moisture reduces S_{95} and β_{VPD} of all species and at all sites, but that (2) species with a more isohydric stomatal behaviour (*P. abies* and *P. sylvestris*) exhibit a higher β_{VPD} at a given S_{95} than more anisohydric species (*Q. ilex* and *F. sylvatica*). We also expect that (3) trees in warmer and drier sites adjust by consistently downregulating S_{95} and β_{VPD} independently of SWC, i.e., they are structurally adapted to low transpiration rates. Lastly, we expected that (4) because of lower soil water competition, less dense stands exhibit higher S_{95} and higher β_{VPD}.

Materials and Methods

Sites and tree species selection

We downloaded the global SAPFLUXNET database, version 0.1.5 (Poyatos et al., 2021), and selected sites where measurements of soil water content (SWC), vapour pressure deficit (VPD), and photosynthetic photon flux density (PPFD) were available concurrently with sap flux density (SFD; sap flow per unit sapwood area). At several sites, SWC was measured manually at low temporal resolution rather than automatically at high resolution. In these cases, data were linearly interpolated to fill gaps no longer than two weeks. We excluded sites where experimental manipulations of environmental conditions were applied, such as thinning, N-fertilisation, CO_2-fertilisation, rainfall throughfall exclusion, or irrigation. We then selected tree species present in at least three sites where three or more dominant, codominant, or subdominant tree individuals of the target species were present per site. Four tree species were selected: *Fagus sylvatica* L., *Picea abies* (L.) H. Karst., *Pinus sylvestris* L., and *Quercus ilex*

L., which were present in 4, 8, 13, and 5 sites, respectively (Fig. 2). At most sites, only one species occurred, but on 5 sites *P. abies* co-occurred with *P. sylvestris* (Table S1). We obtained measurements from 32, 65, 147, and 52 tree individuals, respectively, amounting to 296 trees from 25 sites (Table S1). To relate SFD to whole-tree functional traits, we obtained measurements of leaf area, sapwood area, and Huber values (*Hv*) that were available in the SAPFLUXNET database (*P. abies*, *P. sylvestris,* and *Q. ilex*).

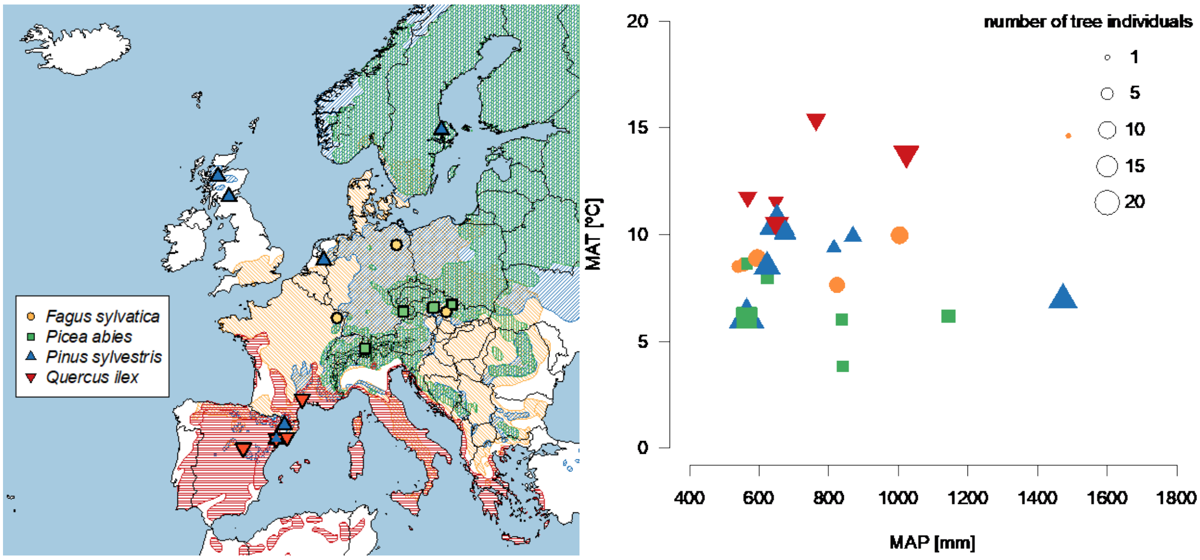

Fig. 2: (a) Distribution of the four selected species and location of the 25 SAPFLUXNET sites in Europe that were selected for this study and (b) Mean annual temperature (MAT) and mean annual precipitation sum (MAP) at the selected sites. The size of the symbols represents the number of individual trees at each site.

Sap flux data processing

From each tree, at each site, we obtained sub-daily (every 10 minutes or half-hourly) sap flux density (SFD) or sap flow (SF) if the sapwood area (A_{SW}) was not available. The SF data were transformed into SFD by dividing SF values by A_{SW} estimated with an allometric approach. For the allometric approach, we used the SAPFLUXNET trees for which the diameter at breast height (DBH) and A_{SW} were provided and calculated the species-specific log-log relationship between these two variables (Fig. S1). The sub-daily SFD, SWC, VPD, and PPFD time series were aggregated, and daytime medians (09:00–16:00) were calculated using the *sfn_metrics* function from the purposely developed *sapfluxnetr* R package (Granda et al., 2020). Measurements obtained from non-calibrated thermal dissipation sensors were corrected for bias multiplying by 1.405, according to a global synthesis of sap flow calibrations (Flo et al., 2019).

Sap flux data filtering

To minimise the influence of phenological changes in leaf area index on SFD, we excluded periods with phenological changes during the cold seasons of each species at each site by removing data for periods between two weeks (14 days) before the first day with temperatures below 0ºC and four weeks (28 days) after the last day with temperatures below 0ºC, similarly to Flo et al. (2021) and Novick et al. (2016). We used temperature thresholds, because the phenological sensitivity to temperature remains relatively stable across different populations of a species (Vitasse et al. 2009). We also removed days where the average daytime VPD was below 0.1 kPa, and rainy days by filtering out days with precipitation (sum of daily precipitation > 0 mm), where measurements were available. If precipitation measurements were lacking, we filtered out days when SWC increased, assuming the increase was due to precipitation, similarly to Flo et al. (2021). As low light is expected to influence stomatal response to SWC and VPD (Oren et al., 1999), we selected days in which the 24-h average photosynthetic photon flux density (PPFD) was greater than 500 μmol m^{-2} s^{-1}, similar to Anderegg et al. (2018).

Sensitivity to VPD and SWC

To calculate the transpiration sensitivity to VPD under different soil water contents, we split the data into five SWC quantiles at each site and fitted five separate linear regressions for each species at each site. We considered that trees are hydraulically adjusted to site conditions (e.g. rooting depth, *Hv*), therefore relative changes in SWC instead of absolute differences will drive tree transpiration. Furthermore, by using SWC quintiles we avoided that extreme values (extremely dry or extremely wet soil) had a too large influence on the regression. We chose to use five quantiles in order to be comparable to existing literature (Novick et al. 2016, Denham et al., 2021), to be able to identify both linear and non-linear (e.g. quadratic) relationships, and to have sufficient datapoints in each quintile for robust regressions.

We applied mixed-effects zero-intercept regression models (LMM) with SFD as the dependent variable, the log-transformed VPD as a fixed factor, and the tree individuals at each site as random slopes. We selected a log-linear regression, as we did not observe a decrease in SFD as VPD increased in the daytime-aggregated data, so they followed a log-linear shape. The VPD was log-transformed to ensure normal distribution of residuals. The LMMs were fitted using the *lmer* function from the *lme4* package (Bates et al., 2014). We obtained the SFD sensitivity to VPD (β_{VPD}) model coefficient for each SWC quintile of each species and site. In addition, we calculated for each site and SWC quintile the maximum SFD (S_{95}) as the 95% percentile of the SFD distribution, and the relative SFD sensitivity to VPD (β_{VPD} / S_{95}). The effect of SWC on β_{VPD}, S_{95}, and β_{VPD} / S_{95} was tested separately for each species with a mixed-effects model, where the SWC quintile was treated as an ordered factor and used as a fixed effect, and the site was considered a random effect. To compare β_{VPD}, S_{95}, and β_{VPD} / S_{95} between species, we used the same mixed-effect model, but for all species combined, and added the species as a fixed effect together with SWC, and the site as random effect. Differences in the SWC effects between species and sites were calculated with the *lstrends* function from the *emmeans* package.

Effect of site soil, climatic, and stand characteristics on sap flux

We tested the effect of several site-specific soil and climate variables and stand characteristics on tree-level β_{VPD} and S_{95}, as well as β_{VPD} / S_{95} across all five SWC quintiles of all the species with multiple linear regression models. The assumptions of homoscedasticity were assessed visually and were met in all cases. In particular, we tested how mean annual temperature (MAT), mean annual precipitation sum (MAP), mean annual precipitation over potential evapotranspiration (P:PET), precipitation seasonality (standard deviation of the monthly deviation from the annual average) and annual temperature range, as well as stand-level basal area, leaf area index (LAI), mean tree height, clay, and sand content of the soil affect β_{VPD} and S_{95}. All long-term means of climatic variables were obtained from the interpolated climate data set CHELSA that covers a time period from 1979–2013 (Karger et al., 2017), whereas basal area, LAI, tree height, clay and sand content are available in the SAPFLUXNET database and were provided by the site managers. We tested the combined effects of the site characteristics by including all variables in a multiple linear regression model and treating the species as random effect. We excluded average tree age from the explanatory variables, as it was too highly correlated with other stand characteristics (e.g. stand height). We then performed a model selection based on the Akaike information criterion (AIC) using the *step* function in R (R Core Team, 2016) to retrieve the most influential variables. To determine the relative importance of the selected variables in explaining β_{VPD} and S_{95}, we performed variance partitioning using the *yhat* package, which can separate contributions to explained variance in the presence of multicollinearity (Ray-Mukherjee et al., 2014). The ability to correct multicollinearity effects on variance partitioning was particularly important for calculating the explained variance of MAP, MAT and P:PET, because the latter is calculated from the former two and thereby not fully independent. In addition to the analysis across SWC quintiles, we selected the driest and wettest SWC quintiles from all sites and repeated the procedure to identify if the same climatic and stand characteristics drive β_{VPD} and S_{95} during days where soils are dry or wet.

Results

Transpiration response to VPD and SWC changes across species

VPD is a strong driver of transpiration, explaining on average 60.3%, 76.5%, 63.6%, and 54.6% of the variance (marginal R^2) of the averaged daytime SFD of *F. sylvatica*, *P. abies*, *P. sylvestris,* and *Q. ilex*, respectively. SFD increased with higher VPD in all species and SWC quintiles (positive β_{VPD}, Fig. 3). The tree species differed in β_{VPD}, with *F. sylvatica* generally having the highest β_{VPD} (Fig. 3, $p < 0.001$). The β_{VPD} significantly increased with the SWC quintile in *F. sylvatica*, *P. sylvestris,* and *Q. ilex* ($p = 0.010$, $p = 0.005$ and $p < 0.001$, respectively; Fig. 3, Table 1) while for *P. abies* SWC quintile showed no effect on β_{VPD} ($p = 0.515$). Pairwise comparisons between species showed that SWC quintile had a more pronounced effect on β_{VPD} (i.e. steeper linear relationship) in *F. sylvatica* and *Q. ilex* than *P. abies* and *P. sylvestris* (Table 2). Pairwise comparisons between sites showed a consistent SWC effect, with the exception of *P. abies* at SWE_NOR_ST5_REF that showed a significantly stronger SWC effect on β_{VPD} compared to other sites, and *P. sylvestris* at GBR_DEV_CON where SWC had a negative effect on β_{VPD}.

The maximum SFD (S_{95}) reached on average 27.1, 8.9, 7.3, and 18.3 $cm^3\ cm^{-2}\ h^{-1}$ across all SWC quintiles and sites for *F. sylvatica*, *P. abies*, *P. sylvestris,* and *Q. ilex*, respectively. Similarly, as with β_{VPD}, S_{95} significantly increased with SWC quintile in *F. sylvatica*, *P. sylvestris,* and *Q. ilex* ($p < 0.001$, $p = 0.010$ and $p = 0.002$, respectively; Fig. 3, Table 1), but not in *P. abies* ($p = 0.476$). Pairwise comparisons between sites showed also a consistent WSC effect on S_{95} except for *P. abies* at SWE_NOR_St4_BEF where SWC had a negative effect on S_{95}. β_{VPD} and S_{95} were positively correlated among populations of the same species ($p < 0.001$), independently of SWC quintiles ($p > 0.05$; Fig. 4). The slope between β_{VPD} and S_{95} differed between species, with *P. sylvestris* having the steepest slope, followed by *P. abies*, *F. sylvatica,* and *Q. ilex*. All slopes differed significantly ($p < 0.05$), except *P. abies* that was not different from *P. sylvestris* and *F. sylvatica*. Leaf area and *Hv* did not affect β_{VPD} and S_{95} across species and populations (Fig. S2).

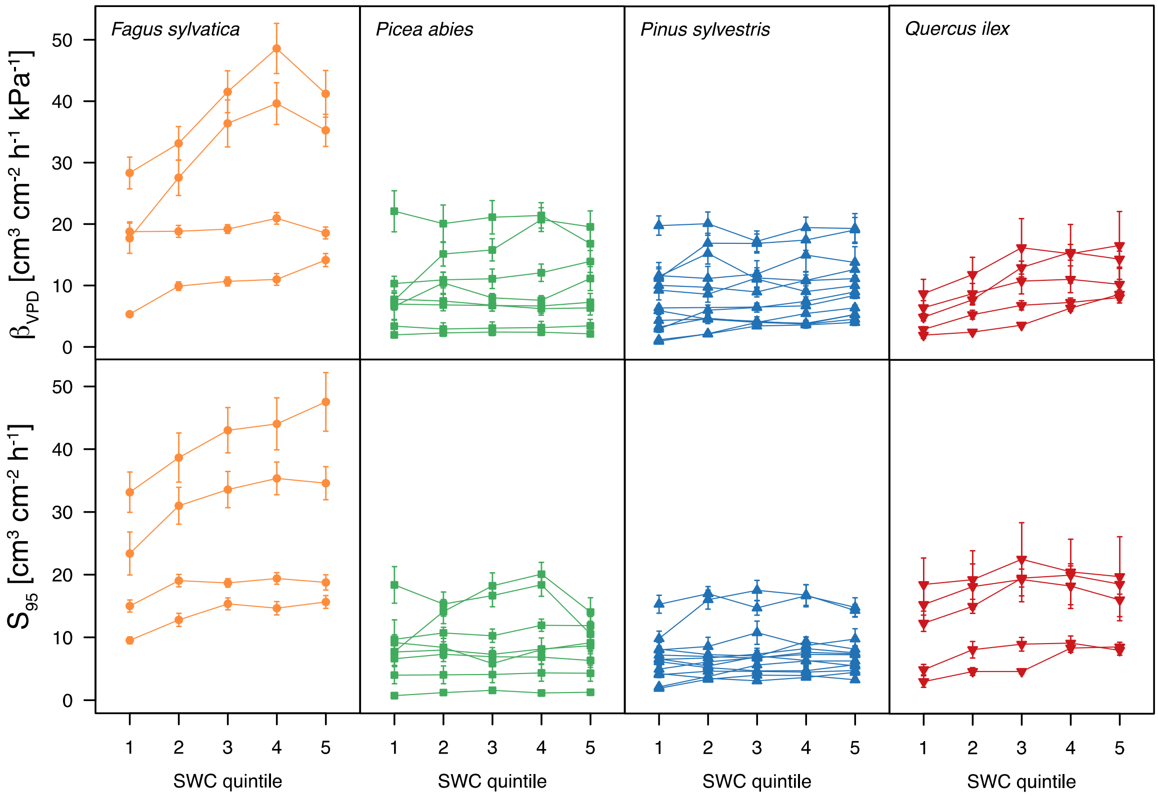

Fig. 3: Sap flux density (SFD) sensitivity to VPD (β_{VPD}) and maximum SFD (S_{95}) in relation to the soil water content (SWC) quintiles at each site for the four species. Error bars represent the standard error of the linear regressions of SFD in relation to VPD of each site and SWC quintile.

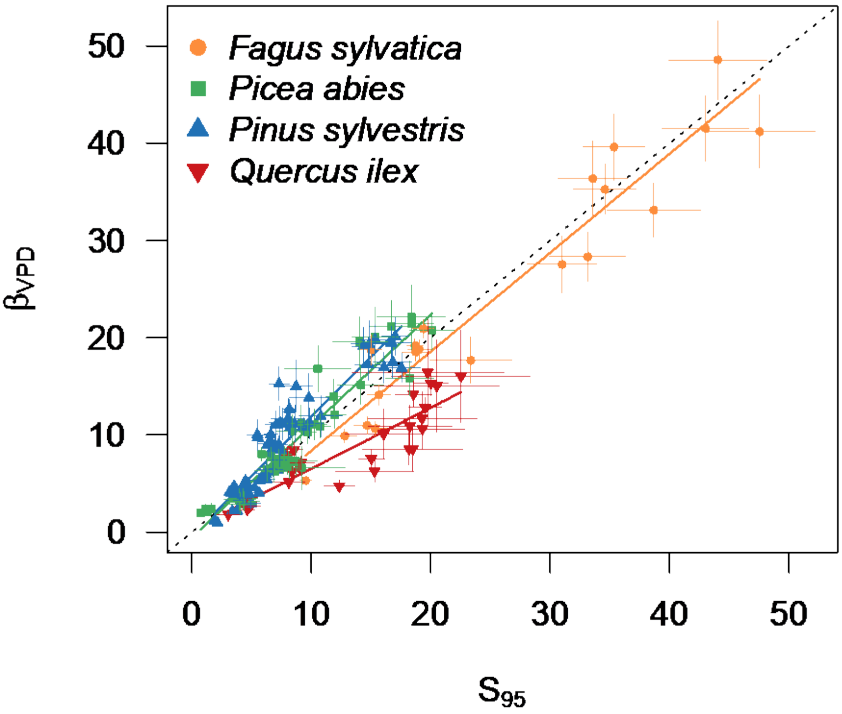

Fig 4: Sap flux density sensitivity to VPD (β_{VPD}) in relation to the maximum sap flux density (S_{95}) of the four species at each site and in all SWC quintiles. Error bars represent the standard error of the linear regressions of SFD in relation to VPD of each site and SWC quintile.

Table 1: Linear mixed model effects of SWC quintiles on SFD sensitivity to VPD (β_{VPD}) and maximum SFD (S_{95}) of the four species. Sites were treated as random effects.

Dependent variable	Species	Mean Sq	Num DF	Den DF	F-value	P-value
β_{VPD}	*F. sylvatica*	97.066	4	12	5.382	0.010
	P. abies	3.969	4	28	0.835	0.515
	P. sylvestris	9.471	4	47	4.275	0.005
	Q. ilex	39.362	4	16	18.527	< 0.001
S_{95}	*F. sylvatica*	51.283	4	12	12.066	< 0.001
	P. abies	4.175	4	28	0.903	0.476
	P. sylvestris	4.005	4	47	2.718	0.041
	Q. ilex	16.314	4	16	7.471	0.001

Table 2: Pairwise comparison of the effect of SWC quintiles on β_{VPD} between species. Coefficients are differences in slope parameters, where significantly positive differences

indicate that in the species in the first column, the SWC quintile had a larger impact on β_{VPD} than in species shown in the top row, and vice versa.

Species	*Picea abies*	*Pinus sylvestris*	*Quercus ilex*
Fagus sylvatica	**2.320; p < 0.001**	**2.214; p < 0.001**	1.014; p = 0.169
Picea abies		-0.106; p = 0.988	**-1.305; p = 0.012**
Pinus sylvestris			**-1.200; p = 0.012**

Climate, stand characteristics, and soil properties influence tree transpiration regulation across populations

Across all SWC quintiles, β_{VPD} was related to several site climatic variables and stand characteristics (Fig. 5). Basal area explained the largest fraction of variability in β_{VPD} with 29.9%, whereas the other site characteristics (mean tree height, MAT, P:PET) explained less than 3% each. In contrast, MAP, precipitation seasonality, annual temperature range, LAI, clay, and sand soil content had no significant effect on β_{VPD}. Most notably, β_{VPD} strongly decreased with higher basal area and the average tree height across species and sites. MAT and P:PET also negatively affected β_{VPD}, indicating that a higher temperature and mean annual water availability reduced the SFD sensitivity to VPD (Table 3). For S_{95}, we observed very similar effects, with the basal area and mean height having a large negative effect on S_{95} across species and populations (Fig. 5). In contrast to β_{VPD}, we found strong evidence that the annual temperature range positively affects S_{95}. Again, basal area explained the largest fraction of variance with 30.7%, whereas mean height and annual temperature range explained 5.6 and 9.5% of the variance, respectively (Table 3). The relative sap flux density (β_{VPD} / S_{95}) was not affected by basal area but decreased with annual temperature range (28.7%), increased with tree height (21.6%), and LAI (5.9% explained variance; Fig. S3).

SFD during wettest and driest SWC quintiles in relation to site characteristics

During the 20% wettest days, β_{VPD} was related to the same site characteristics across all SWC quintiles (Table 4). Basal area was the most influential driver of β_{VPD} (28.2%), followed by MAT (6.2%), P:PET (2.3%), and mean height (1.3%). Similarly, S_{95} was related to the basal area, mean height, and annual temperature range. In addition to the analysis across SWC quintiles, the soil's clay fraction was an additional factor driving S_{95}. During the 20% driest days, β_{VPD} and S_{95} strongly decreased with soil clay and sand fractions (Table 4). While in both cases the negative effect of basal area remained the most critical driver of SFD responses (β_{VPD}: 25.9%, S_{95}: 35.2%), the two soil characteristics explained a considerable fraction of the variance (β_{VPD}: 11.9% and 14.1% for clay and sand; S_{95}: 8.2% and 14.8% for clay and sand). Maximum SFD was also marginally related to precipitation seasonality ($p = 0.05$), which explained 17.2% of S_{95} during the driest 20% of days.

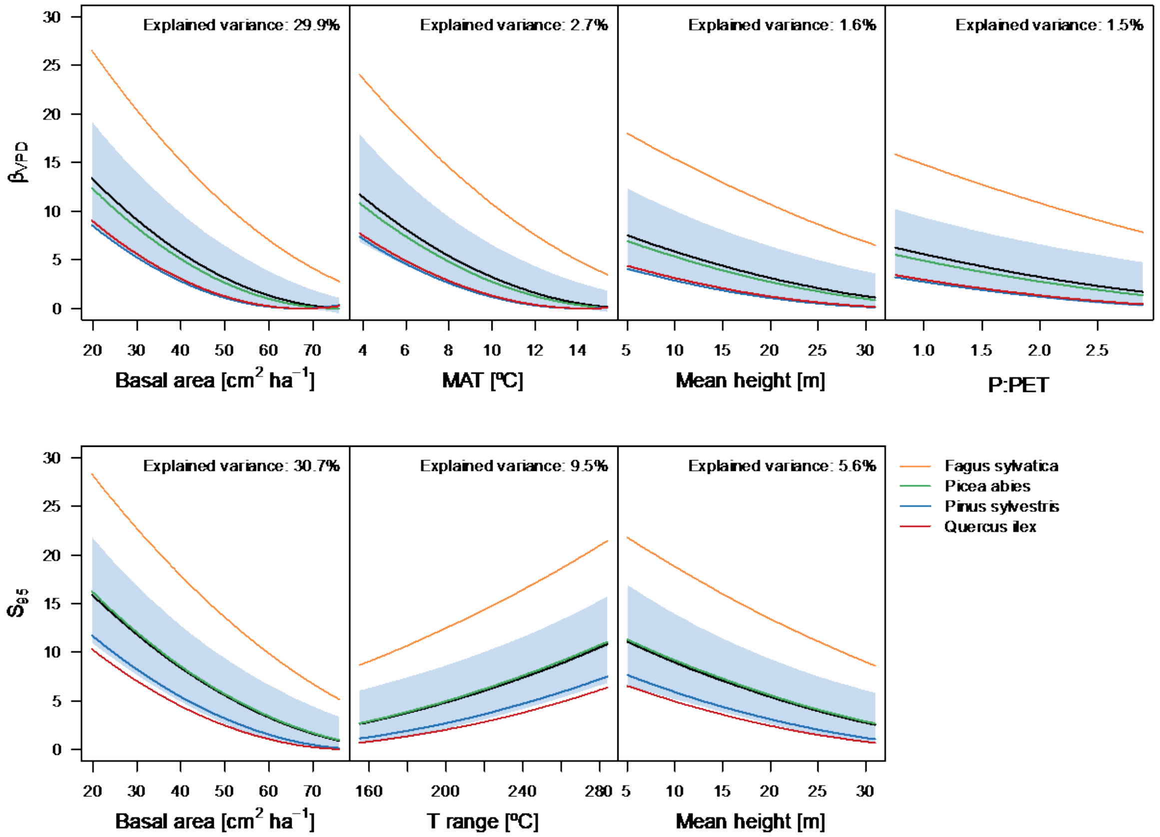

Fig 5: Partial regression of sap flux sensitivity to VPD (β_{VPD}) and maximum sap flux density (S_{95}) in relation to climatic and stand characteristics of all sites, across the four species and the

five SWC quintiles (black lines). Species-specific regressions were obtained from the random intercepts. Only the climatic and stand characteristics that were significant in the multiple regression model are shown (see Table 3). The blue bands show the prediction intervals of the fixed effects.

Table 3: Linear mixed model effects of stand characteristics and climate on SFD sensitivity to VPD (β_{VPD}) and maximum SFD (S_{95}) across all SWC quintiles. Species were treated as random effects.

Dependent variable	Explanatory variable	Estimate	Std. Error	DF	T-value	P-value	Explained variance
β_{VPD}	Basal area	-0.062	0.009	19.329	-7.259	< 0.001	0.299
	Mean height	-0.065	0.019	19.323	-3.432	0.003	0.016
	MAT	-0.264	0.068	20.468	-3.869	0.001	0.027
	P:PET	-0.557	0.186	19.065	-2.996	0.007	0.015
S_{95}	Basal area	-0.054	0.010	20.513	-5.208	< 0.001	0.307
	Mean height	-0.067	0.021	21.609	-3.136	0.005	0.056
	Temp range	0.013	0.004	20.275	3.701	0.001	0.095
β_{VPD} / S_{95}	Temp range	-0.007	0.001	18.282	-4.890	< 0.001	0.287
	Mean height	0.023	0.006	9.414	3.826	0.004	0.216
	LAI	0.073	0.031	14.337	2.394	0.031	0.059

Table 4: Linear mixed model effects of stand characteristics and climate on SFD sensitivity to VPD (β_{VPD}) and maximum SFD (S_{95}) during driest (Q1) and moistest (Q5) quintiles of SWC of each site. Species were treated as random effects.

SWC Quintile	Dependent variable	Explanatory variable	Estimate	Std. Error	DF	T-value	P-value	Explained variance
driest (Q1)	β_{VPD}	Basal area	-0.061	0.010	14.6	-5.840	< 0.001	0.259
		Clay %	-0.276	0.062	5.4	-4.454	0.006	0.119
		Sand %	-0.127	0.029	5.5	-4.407	0.005	0.141
	S_{95}	Basal area	-0.055	0.010	20.0	-5.766	< 0.001	0.352
		Clay %	-0.210	0.053	11.6	-3.959	0.002	0.082
		Sand %	-0.113	0.025	10.6	-4.594	0.001	0.148
		Precip seasonality	-0.035	0.017	21.7	-2.079	0.050	0.172
	β_{VPD} / S_{95}	MAT	-0.105	0.030	24	-3.491	0.002	0.279
		Temp range	-0.004	0.002	24	-2.168	0.040	0.079
moistest (Q5)	β_{VPD}	Basal area	-0.055	0.008	19.3	-7.030	< 0.001	0.282
		Mean height	-0.095	0.017	19.3	-5.446	< 0.001	0.013
		MAT	-0.275	0.063	20.2	-4.391	< 0.001	0.062
		P:PET	-0.649	0.170	19.1	-3.814	0.001	0.023

S_{95}	Basal area	-0.036	0.009	19.5	-3.821	0.001	0.276
	Mean height	-0.085	0.021	19.4	-4.113	0.001	0.051
	Temp range	0.017	0.004	19.2	3.988	0.001	0.048
	Clay %	-0.047	0.022	20.0	-2.158	0.043	0.079
β_{VPD} / S_{95}	MAT	-0.044	0.019	24	-2.364	0.027	0.11
	Temp range	-0.004	0.001	24	-3.019	0.006	0.21

Discussion

Transpiration responses to VPD vary with SWC across species

SFD sensitivity to VPD (β_{VPD}) was strongly related to the soil water availability in *F. sylvatica*, *Q. ilex*, and to a lesser degree in *P. sylvestris* (Table 1, Fig. 3). As hypothesized, days with lower SWC reduced β_{VPD} and maximum SFD (S_{95}) in these species (Fig. 3). These findings confirm that water demand and supply co-determine tree transpiration and that SWC strongly modulates stomatal sensitivity to VPD (e.g., Grossiord et al., 2018). Despite the wide range of absolute soil water contents, the relationship between β_{VPD} and S_{95} and the SWC quintiles was consistent across sites (Fig. 3), with the exception of three sites, where *P. abies* and *P. sylvestris* showed stronger or contrasting SWC effects. The consistent SWC effect indicates that relative, not absolute changes in soil moisture was determining the transpiration of the locally adjusted trees. Thus, using SWC quintiles, instead of absolute values of SWC proved to be beneficial in tracking tree transpiration responses to soil moisture. In addition to these general patterns, we observed large species-specific differences in the transpiration responses to VPD and SWC, with evergreen species showing overall lower S_{95} and β_{VPD} compared to the deciduous *F. sylvatica* (Fig. 3). While β_{VPD} and S_{95} of the two broadleaves were strongly co-determined by SWC, the two conifers showed no, or only a weak response to SWC (Fig. 3). The large species-specific differences were expected due to their affiliation to different functional types and hydraulic traits (Flo et al., 2021; Grossiord et al., 2018; Hassler et al., 2018; Peters et al., 2019). By relating β_{VPD} to S_{95}, we observed that the two conifers showed higher sensitivity at a given

S_{95} than the broadleaves (Fig. 4). The relative sap flux sensitivity to VPD (β_{VPD} / S_{95}) was positively related to the SWC quintile for *P. sylvestris* and *Q. ilex* ($p < 0.05$) but not for the other two species (Fig. S4). The differences in relative sensitivities can be explained by contrasting stomatal regulation in response to water potential, as indicated by the leaf water potential at the turgor loss point (Ψ_{TLP}). Accordingly, the least sensitive species, *Q. ilex,* has the lowest Ψ_{TLP} (-3.2 MPa), followed by *F. sylvatica* (-2.5 MPa), *P. abies* (-2.5 MPa), and *P. sylvestris* (-2.1 MPa) (Martin-StPaul et al., 2017). Similarly, their isohydricity aligns along the same order (hydroscape area; Fu & Meinzer, 2018) with *Q. ilex* (3.18) as the most anisohydric species having the lowest β_{VPD} at a given S_{95}, followed by *F. sylvatica* (2.49), *P. abies* (2.11) and *P. sylvestris* (1.95). Hence, in contrast to recent findings where similar responses of several tree species to VPD were found along an isohydric range (Denham et al., 2021), we observed a strong species effect consistent with hydraulic traits.

Adjustment to climate modifies VPD and SWC effects on transpiration

Across species, adjustment to climate led to lower β_{VPD} in trees growing in warmer and moister sites (higher P:PET), whereas a larger annual temperature range, i.e. a higher continentality of the site, increased S_{95} (Fig. 5). Consequently, the relative sap flux sensitivity to VPD (β_{VPD} / S_{95}) was lower in more continental sites (Fig. S3). The observed adjustment to warm temperatures is consistent with previous work where *Pinus edulis* and *Juniperus monosperma* acclimated to warmer climate by reducing the sensitivity of SFD to VPD even under high soil moisture (Grossiord et al., 2018). These findings indicate a long-term downregulation of tree-level transpiration under warmer climate to maintain hydraulic functioning ('downregulation' scenario, Fig. 1). Reduced β_{VPD} at moister sites (higher P:PET) is contrary to our third hypothesis, as we expected a downregulation combined with reduced sensitivity at xeric sites. However, it supports observations of a long-term irrigation experiment with *P. sylvestris* that showed lower tree transpiration sensitivity to VPD of trees acclimated to humid soils (Schönbeck et al., 2022). Furthermore, it is consistent with a recent study by Denham et al. (2021), who found higher transpiration sensitivity to VPD of trees in xeric compared to mesic sites. At first glance, this contradicts the observation that days with lower SWC reduced β_{VPD} (Fig. 3). We observed, however, that only during times of high water availability (Q5) β_{VPD} was reduced by a high P:PET (Table 4), which implies a more competitive strategy of tree water use in these conditions. As soils dry out (Q1) β_{VPD} becomes similar across the P:PET gradient. Our observations are partly in contrast with Novick et al. (2016), who found a positive effect of site soil dryness on stand-level transpiration sensitivity to VPD, however, mainly in savannahs and grasslands, while forests showed no clear adjustments to soil humidity. Our observations also contrast with Poyatos et al. (2007), who showed increased sap flow sensitivity to VPD and SWC in *P. sylvestris* in warmer sites with drier soils, although no hot and dry sites were included (Sus et al., 2014).

Across species, the sensitivity to VPD is related to hydraulic traits, such as vulnerability to embolism, *Hv*, hydraulic conductivity, turgor-loss point, rooting depth, and leaf size (Flo et al., 2021). Similarly, within a single species, Poyatos et al. (2007) found a significant effect of tree-level *Hv* on sensitivity parameters of transpiration to VPD. While detailed plant trait measurements were lacking for most sites, we obtained leaf area, sapwood area, and *Hv* for *P. abies*, *P. sylvestris,* and *Q. ilex*. We found, however, no effect of leaf area and *Hv* on β_{VPD} and S_{95} across species and populations (Fig. S2), whereas the relative sap flux sensitivity to VPD was positively related to leaf area across species and populations ($p = 0.018$). Overall, our findings partly validate our third hypothesis: populations from warmer sites adjusted to higher temperatures by downregulating their transpiration sensitivity to VPD, indicating that they are structurally adjusted for reduced transpiration rates. However, in contrast to our third hypothesis, lower climatic water availability, which could translate to higher soil drought, had a slightly positive effect on transpiration rates. The different adjustments of VPD sensitivity to long-term soil water and air temperature therefore call for further in-depth analysis of the adjustment mechanisms to soil *vs.* atmospheric droughts. Furthermore, earlier cross-species analyses of climate adjustments could not incorporate species-specific responses due to data scarcity. Therefore, whether adjustments to environmental gradients and stand characteristics vary from species to species could not be ascertained.

Stand structure drives transpiration responses to VPD and SWCI

We observed that across species β_{VPD} and S_{95} were mainly driven by stand basal area, which explained around 30% of their variability across soil moisture levels and during days with dry and wet soils (Tables 3 and 4). We excluded experimentally thinned plots to avoid measuring short-term responses of tree transpiration to changes in stand characteristics. Nevertheless, studies assessing thinning effects might help identify the mechanisms underlying stand structure effects on transpiration responses to the environment as they assess the impact of stand density and basal area reductions under a given climate and soil type. Thinning induces changes in light availability, airflow within the canopy, and soil water availability through reduced water consumption and interception by the canopy (Gebhardt et al., 2014; Moore et al., 2004). Thus, changes in stand structure affect tree water relations in two ways: through changes in the aboveground microclimate and changes in belowground water availability and competition (Hassler et al., 2018). The higher β_{VPD} and S_{95} of trees growing in stands with lower basal area are most likely related to these effects. The effect of access to extractable soil water was evident during days with low soil moisture, where high clay and sand contents (and correspondingly a low silt content) were reducing β_{VPD} and S_{95} (Table 4). This confirms previous observations on the importance of soil type on tree transpiration (Hassler et al., 2018; Tromp-van Meerveld & McDonnell, 2006). Canopy microclimate further strongly impacted transpiration as indicated by a strong effect of basal area on β_{VPD} when soil water access was not limiting (Table 4). In stands with higher basal area, the water exchange from the leaf to the atmosphere is hampered because the atmosphere around leaves in the canopy is not well coupled to the atmosphere above the forest stand (Paul-Limoges et al., 2017; Zhang et al., 2016). This lowers transpirational water loss of individual trees, resulting in a microclimate with lower VPD at the bottom canopy layers than the canopy top (Bachofen et al., 2020). Consequently, the sensitivity of stomata to changes in VPD is dampened in high basal area stands compared to low basal area stands (Song et al., 2020; Zhang et al., 2016). Correspondingly, trees in low-basal area forests exhibit a higher VPD sensitivity, which might increase their susceptibility to extremely hot conditions and soil drought (Song et al., 2020). Stand basal area can also be correlated with the ontogenetic state of the forest and, thus, be partly confounded with tree height and stand LAI (Fig. S5). By including these variables in the linear mixed model, we are confident that stand basal area was the most important driver of tree transpiration sensitivity to VPD. The average tree age of the forest stands was highly correlated with other stand characteristics, particularly stand height, thus specific age effects could not be disentangled from the effects of basal area, height and LAI. Tree height and LAI were also important drivers of the relative SFD sensitivity to VPD (β_{VPD} / S_{95}; Fig. S3), indicating that multiple site characteristics drive tree transpiration in conjunction. In addition, low stand basal area can be related to high sapwood area per tree, which has been shown to result in a higher canopy transpiration, and a pronounced transpiration sensitivity to climate and soil drought (Chen et al., 2020). Hence, our work suggests that tree transpiration response to VPD can be effectively regulated by controlling stand basal area. The beneficial effect of an open stand on soil moisture contrasts with the effect it has on the susceptibility to hot conditions and soil drought. Therefore, the advantages and disadvantages of low-basal area stands need to be evaluated locally by considering the major limitations of tree transpiration.

Conclusions and implications for forest management

We observed that tree transpiration is sensitive to changes in soil and atmospheric water availability that happen on a short time scale (daily), and that trees adjust to site climatic and edaphic conditions that vary on a longer time scale (decades). The consistent observations of a downregulation of transpiration and its sensitivity to VPD with higher air temperatures have important implications on the global water cycle because of the role of tree transpiration on global water exchange (Schlesinger & Jasechko, 2014). Regional forest transpiration can be directly linked with precipitation in the vicinity, creating a positive feedback between transpiration and precipitation (Spracklen et al., 2012; Staal et al., 2018). Thus, transpiration downregulation under a warmer climate could reduce water exchange with the atmosphere (Grossiord et al., 2019), leading to negative feedback and lower precipitation. Basal area was the main driver of maximum tree transpiration and the sensitivity of tree transpiration to VPD. Hence, forest management practices can tremendously impact tree transpiration. In Europe, land-use changes since the 1950s, including the abandonment of agroforestry practices, have led to nearly doubling stand densities (Fuchs et al., 2013; Gold et al., 2006). Consequently, resource competition among trees increased (Giuggiola et al., 2018). Stand thinning can generally increase the water availability for the remaining trees (Flathers et al., 2016; Giuggiola et al., 2016), but it might also increase the susceptibility of remaining trees to heat and soil drought events (Song et al., 2020) with contrasting responses of tree species according to their transpiration responses to VPD and soil water conditions (Fig. 3). Any interventions in stand structure thus need to be considered in the specific context, including the climatic and edaphic conditions.

Authors' contribution

The study was conceived and designed by Christoph Bachofen, Charlotte Grossiord, Rafael Poyatos, Jordi Martínez-Vilalta, Víctor Flo, and Maurizio Mencuccini. Víctor Flo, Víctor Granda, and Rafael Poyatos set the database. Christoph Bachofen carried out the statistical

analyses with support from Charlotte Grossiord and Rafael Poyatos and led the writing of the manuscript. All authors contributed critically to the draft and approved publishing the final version.

Conflict of interest

The authors declare that they have no conflict of interest or personal relationships that could have influenced this work.

Acknowledgements

Christoph Bachofen and Charlotte Grossiord were supported by the Swiss National Science Foundation (IZSEZ0_197453, PZ00P3_174068, 310030_204697). Rafael Poyatos acknowledges support from the Spanish State Research Agency (DATAFORUSE, RTI2018-095297-J-I00) and the Alexander von Humboldt Foundation (Germany). The Spanish Ministry of Universities supported Víctor Flo through a Margarita Salas grant (698511). Our study was based on data from a worldwide sap flux database and did not involve generating new data. Therefore, there was no local data collection. However, the geographical distribution of the authors broadly represents the regions of interest of the analyses (Europe). As such, it supports the inclusion of data from all relevant sites across the study region, ensuring the appropriate interpretation of data and results from each region.

Data availability statement

All data of the SAPFLUXNET (version 0.1.5) are freely available from the Zenodo repository at https://doi.org/10.5281/zenodo.3971689 (Poyatos et al. 2020).

References

Addington, R.N., Donovan, L.A., Mitchell, R.J., Vose, J.M., Pecot, S.D., Jack, S.B., Hacke, U.G., Sperry, J.S., & Oren, R. (2006). Adjustments in hydraulic architecture of Pinus palustris maintain similar stomatal conductance in xeric and mesic habitats. *Plant, Cell and Environment*, *29*(4), 535–545.

Anderegg, W.R.L., Konings, A.G., Trugman, A.T., Yu, K., Bowling, D.R., Gabbitas, R., Karp, D.S., Pacala, S., Sperry, J.S., Sulman, B.N., & Zenes, N. (2018). Hydraulic diversity of forests regulates ecosystem resilience during drought. *Nature*, *561*(7724), 538–541.

Bachofen, C., D'Odorico, P., & Buchmann, N. (2020). Light and VPD gradients drive foliar nitrogen partitioning and photosynthesis in the canopy of European beech and silver fir. *Oecologia*, *192*(2), 323–339.

Bates, D., Mächler, M., Bolker, B., & Walker, S. (2014). Fitting Linear Mixed-Effects Models using lme4 [Computation]. *Journal of Statistical Software*, 51.

Caballé, G., Fernández, M.E., Gyenge, J., Lantschner, V., Rusch, V., Letourneau, F., & Borrelli, L. (2016). Silvopastoral Systems Based on Natural Grassland and Ponderosa Pine in Northwestern Patagonia, Argentina. In P.L. Peri, F. Dube, & A. Varella (Eds.), *Silvopastoral Systems in Southern South America, Advances in Agroforestry* (Vol. 11, pp. 63–87). Springer.

Chen, Z., Zhang, Z., Chen, L., Cai, Y., Zhang, H., Lou, J., Xu, Z., Xu, H., & Song, C. (2020). Sparse pinus tabuliformis stands have higher canopy transpiration than dense stands three decades after thinning. *Forests*, *11*(1), 1–18.

Cochard, H., Coll, L., Le Roux, X., & Améglio, T. (2002). Unraveling the effects of plant hydraulics on stomatal closure during water stress in walnut. *Plant Physiology*, *128*(1), 282–290.

D. Whitehead, Jarvis, P.G., & Waring, R.H. (1984). Stomatal conductance, transpiration, and resistance to water uptake in a Pinussylvestris spacing experiment. *Canadian Journal of Forest Research*, *14*(5).

Dai, A. (2006). Recent climatology, variability, and trends in global surface humidity. *Journal of Climate*, *19*(15), 3589–3606.

Denham, S.O., Christopher Oishi, A., Miniat, C.F., Wood, J.D., Yi, K., Benson, M.C., & Novick, K.A. (2021). Eastern US deciduous tree species respond dissimilarly to declining soil moisture but similarly to rising evaporative demand. *Tree Physiology*, *41*(6), 944–959.

Ficklin, D.L., & Novick, K.A. (2017). Historic and projected changes in vapor pressure deficit suggest a continental-scale drying of the United States atmosphere. *Journal of Geophysical Research*, *122*(4), 2061–2079.

Flathers, K.N., Kolb, T.E., Bradford, J.B., Waring, K.M., & Moser, W.K. (2016). Long-term thinning alters ponderosa pine reproduction in northern Arizona. *Forest Ecology and Management*, *374*, 154–165.

Flo, V, Martínez-Vilalta, J., Mencuccini, M., Granda, V., Anderegg, W.R.L., & Poyatos, R. (2021). Climate and functional traits jointly mediate tree water use strategies. *New Phytologist*, *2001*, 3–29.

Flo, V, Martinez-Vilalta, J., Steppe, K., Schuldt, B., & Poyatos, R. (2019). A synthesis of bias and uncertainty in sap flow methods. *Agricultural and Forest Meteorology*, *271*(July 2018), 362–374.

Fu, X., & Meinzer, F.C. (2018). Metrics and proxies for stringency of regulation of plant water status (iso/anisohydry): A global data set reveals coordination and trade-offs among water transport traits. *Tree Physiology*, *39*(1), 122–134.

Fuchs, R., Herold, M., Verburg, P.H., & Clevers, J.G.P.W. (2013). A high-resolution and harmonized model approach for reconstructing and analysing historic land changes in

Europe. *Biogeosciences*, *10*(3), 1543–1559. https://doi.org/10.5194/bg-10-1543-2013

Gartner, B.L., & Meinzer, F.C. (2005). Structure-Function Relationships In Sapwood Water Transport And Storage. *Vascular Transport in Plants*, 307–331.

Gebhardt, T., Häberle, K.H., Matyssek, R., Schulz, C., & Ammer, C. (2014). The more, the better? Water relations of Norway spruce stands after progressive thinning. *Agricultural and Forest Meteorology*, *197*, 235–243.

Giuggiola, A, Ogee, J., Gessler, A., Rigling, A., Bugmann, H., & Treydte, K. (2016). Improvement of water and light availability after thinning at a xeric site: Which weighs more? A dual isotope approach. *New Phytologist*, *210*(1), 108–121.

Giuggiola, A, Zweifel, R., Feichtinger, L.M., Vollenweider, P., Bugmann, H., Haeni, M., & Rigling, A. (2018). Competition for water in a xeric forest ecosystem – Effects of understory removal on soil micro-climate, growth and physiology of dominant Scots pine trees. *Forest Ecology and Management*, *409*(February), 241–249.

Gold, S., Korotkov, A., & Sasse, V. (2006). The development of European forest resources, 1950 to 2000. *Forest Policy and Economics*, *8*(2), 183–192.

Granda, E., Baumgarten, F., Gessler, A., Gil-Pelegrin, E., Peguero-Pina, J.J., Sancho-Knapik, D., Zimmerman, N.E., & Resco de Dios, V. (2020). Day length regulates seasonal patterns of stomatal conductance in Quercus species. *Plant, Cell & Environment*, *43*(1), 28–39.

Granda, V., Poyatos, R., Flo, V., & Nelson, J.A. (2020). sapfluxnetr: Working with 'Sapfluxnet' Project Data. *URL Https://Cran.r-Project.Org/Package=sapfluxnetr*.

Grossiord, C., Buckley, T.N., Cernusak, L.A., Novick, K.A., Poulter, B., Siegwolf, R.T.W., Sperry, J.S., & McDowell, N.G. (2020). Plant responses to rising vapor pressure deficit. *New Phytologist*.

Grossiord, C., Christoffersen, B., Alonso-Rodríguez, A.M., Anderson-Teixeira, K., Asbjornsen, H., Aparecido, L.M.T., Carter Berry, Z., Baraloto, C., Bonal, D., Borrego, I.,

… McDowell, N.G. (2019). Precipitation mediates sap flux sensitivity to evaporative demand in the neotropics. *Oecologia*, *191*(3), 519–530.

Grossiord, C., Sevanto, S., Borrego, I., Chan, A.M., Collins, A.D., Dickman, L.T., Hudson, P.J., McBranch, N., Michaletz, S.T., Pockman, W.T., Ryan, M., Vilagrosa, A., & McDowell, N.G. (2017). Tree water dynamics in a drying and warming world. *Plant, Cell & Environment*, *40*(9), 1861–1873.

Grossiord, C., Sevanto, S., Limousin, J.M., Meir, P., Mencuccini, M., Pangle, R.E., Pockman, W.T., Salmon, Y., Zweifel, R., & McDowell, N.G. (2018). Manipulative experiments demonstrate how long-term soil moisture changes alter controls of plant water use. *Environmental and Experimental Botany*, *152*(August 2017), 19–27.

Hassler, S.K., Weiler, M., & Blume, T. (2018). Tree-, stand- and site-specific controls on landscape-scale patterns of transpiration. *Hydrology and Earth System Sciences*, *22*, 13–30.

Karger, D.N., Conrad, O., Böhner, J., Kawohl, T., Kreft, H., Soria-Auza, R.W., Zimmermann, N.E., Linder, H.P., & Kessler, M. (2017). Climatologies at high resolution for the earth's land surface areas. *Scientific Data*, *4*, 1–20.

Klein, T. (2014). The variability of stomatal sensitivity to leaf water potential across tree species indicates a continuum between isohydric and anisohydric behaviours. *Functional Ecology*, *28*(6), 1313–1320.

Liu, J.L., Cheng, F.Y., Munger, W., Jiang, P., Whitby, T.G., Chen, S.Y., Ji, W.W., & Man, X.L. (2020). Precipitation extremes influence patterns and partitioning of evapotranspiration and transpiration in a deciduous boreal larch forest. *Agricultural and Forest Meteorology*, *287*(August 2019), 107936.

Maherali, H., & DeLucia, E.H. (2001). Influence of climate-driven shifts in biomass allocation on water transport and storage in ponderosa pine. *Oecologia*, *129*(4), 481–491.

Marchin, R.M., Broadhead, A.A., Bostic, L.E., Dunn, R.R., & Hoffmann, W.A. (2016).

Stomatal acclimation to vapour pressure deficit doubles transpiration of small tree seedlings with warming. *Plant Cell and Environment*, *39*(10), 2221–2234.

Martin-StPaul, N., Delzon, S., & Cochard, H. (2017). Plant resistance to drought depends on timely stomatal closure. *Ecology Letters*, *20*(11), 1437–1447.

Martínez-Vilalta, J., & Garcia-Forner, N. (2017). Water potential regulation, stomatal behaviour and hydraulic transport under drought: deconstructing the iso/anisohydric concept. *Plant, Cell & Environment*, *40*(6), 962–976.

Martínez-Vilalta, J., Poyatos, R., Aguadé, D., Retana, J., & Mencuccini, M. (2014). A new look at water transport regulation in plants. *New Phytologist*, *204*(1), 105–115.

McCarthy, M.P., Thorne, P.W., & Titchner, H.A. (2009). An analysis of tropospheric humidity trends from radiosondes. *Journal of Climate*, *22*(22), 5820–5838.

McDowell, N.G., Sapes, G., Pivovaroff, A., Adams, H.D., Allen, C.D., Anderegg, W.R.L., Arend, M., Breshears, D.D., Brodribb, T., Choat, B.,… Xu, C. (2022). Mechanisms of woody-plant mortality under rising drought, CO2 and vapour pressure deficit. *Nature Reviews Earth & Environment*, *3*(May), 41–44.

Meinzer, F.C. (2003). Functional convergence in plant responses to the environment. *Oecologia*, *134*(1), 1–11.

Mencuccini, M., Minunno, F., Salmon, Y., Martínez-Vilalta, J., & Hölttä, T. (2015). Coordination of physiological traits involved in drought-induced mortality of woody plants. *New Phytologist*, *208*(2), 396–409.

Monteith, J.L. (1995). A reinterpretation of stomatal responses to humidity. *Plant, Cell & Environment*, *18*(4), 357–364.

Moore, G.W., Bond, B.J., Jones, J.A., Phillips, N., & Meinzer, F.C. (2004). Structural and compositional controls on transpiration in 40- and 450-year-old riparian forests in western Oregon, USA. *Tree Physiology*, *24*(5), 481–491.

Novick, K.A., Ficklin, D.L., Stoy, P.C., Williams, C.A., Bohrer, G., Oishi, A.C., Papuga, S.A., Blanken, P.D., Noormets, A., Sulman, B.N.,… Phillips, R.P. (2016). The increasing importance of atmospheric demand for ecosystem water and carbon fluxes. *Nature Climate Change*, *6*(11), 1023–1027.

Oren, R., Sperry, J.S., Katul, G.G., Pataki, D.E., Ewers, B.E., Phillips, N., & Schäfer, K.V.R. (1999). Survey and synthesis of intra- and interspecific variation in stomatal sensitivity to vapour pressure deficit. *Plant, Cell and Environment*, *22*(12), 1515–1526.

Paul-Limoges, E., Wolf, S., Eugster, W., Hörtnagl, L., & Buchmann, N. (2017). Below-canopy contributions to ecosystem CO_2 fluxes in a temperate mixed forest in Switzerland. *Agricultural and Forest Meteorology*, *247*(August), 582–596.

Peters, R.L., Speich, M., Pappas, C., Kahmen, A., von Arx, G., Graf Pannatier, E., Steppe, K., Treydte, K., Stritih, A., & Fonti, P. (2019). Contrasting stomatal sensitivity to temperature and soil drought in mature alpine conifers. *Plant, Cell & Environment*, *42*(5), 1674–1689.

Poyatos, R., Granda, V., Flo, V., Adams, M.A., Adorján, B., Aguadé, D., Aidar, M.P.M., Allen, S., Alvarado-Barrientos, M.S., Anderson-Teixeira, K.J., … Martínez-Vilalta, J. (2021). Global transpiration data from sap flow measurements: the SAPFLUXNET database. *Earth System Science Data*, *13*(6), 2607–2649.

Poyatos, R., Martínez-Vilalta, J., Cermák, J., Ceulemans, R., Granier, A, Irvine, J., Köstner, B., Lagergren, F., Meiresonne, L., Nadezhdina, N., Zimmermann, R., Llorens, P., & Mencuccini, M. (2007). Plasticity in hydraulic architecture of Scots pine across Eurasia. *Oecologia*, *153*(2), 245–259.

Poyatos, R., Granda, V., Flo, V., Molowny-Horas, R., Steppe, K., Mencuccini, M., & Martínez-Vilalta, J. (2020). Data is available from: SAPFLUXNET: A global database of sap flow measurements (Version 0.1. 5)[Data set], Zenodo, https://doi.org/10.5281/zenodo.3971689

R Core Team. (2016). *R: A Language and Environment for Statistical Computing* (3.2.4). R

Foundation for Statistical Computing. http://www.r-project.org/

Ray-Mukherjee, J., Nimon, K., Mukherjee, S., Morris, D.W., Slotow, R., & Hamer, M. (2014). Using commonality analysis in multiple regressions: A tool to decompose regression effects in the face of multicollinearity. *Methods in Ecology and Evolution*, *5*(4), 320–328.

Running, S.W. (1976). Environmental control of leaf water conductance in conifers. *Canadian Journal of Forest Research*, *6*(104–112).

Schlesinger, W.H., & Jasechko, S. (2014). Transpiration in the global water cycle. *Agricultural and Forest Meteorology*, *189–190*, 115–117.

Schönbeck, L., Grossiord, C., Gessler, A., Gisler, J., Meusburger, K., D'Odorico, P., Andreas, R., Salmon, Y., Stocker, B., Zweifel, R., & Schaub, M. (2022). Photosynthetic acclimation and sensitivity to short- and long-term environmental changes in a drought prone forest. *Journal of Experimental Botany*, 1–26.

Song, L., Zhu, J., Zheng, X., Wang, K., Lü, L., Zhang, X., & Hao, G. (2020). Transpiration and canopy conductance dynamics of Pinus sylvestris var. mongolica in its natural range and in an introduced region in the sandy plains of Northern China. *Agricultural and Forest Meteorology*, *281*(November 2019), 107830.

Spracklen, D.V., Arnold, S.R., & Taylor, C.M. (2012). Observations of increased tropical rainfall preceded by air passage over forests. *Nature*, *489*(7415), 282–285.

Staal, A., Tuinenburg, O.A., Bosmans, J.H.C., Holmgren, M., Van Nes, E.H., Scheffer, M., Zemp, D.C., & Dekker, S.C. (2018). Forest-rainfall cascades buffer against drought across the Amazon. *Nature Climate Change*, *8*(6), 539–543.

Stoy, P.C., El-Madany, T.S., Fisher, J.B., Gentine, P., Gerken, T., Good, S.P., Klosterhalfen, A., Liu, S., Miralles, D.G., Perez-Priego, O., … Wolf, S. (2019). Reviews and syntheses: Turning the challenges of partitioning ecosystem evaporation and transpiration into opportunities. *Biogeosciences*, *16*(19), 3747–3775.

Sus, O., Poyatos, R., Barba, J., Carvalhais, N., Llorens, P., Williams, M., & Vilalta, J.M. (2014). Time variable hydraulic parameters improve the performance of a mechanistic stand transpiration model. A case study of Mediterranean Scots pine sap flow data assimilation. *Agricultural and Forest Meteorology*, *198*, 168–180.

Tromp-van Meerveld, H.J., & McDonnell, J.J. (2006). On the interrelations between topography, soil depth, soil moisture, transpiration rates and species distribution at the hillslope scale. *Advances in Water Resources*, *29*(2), 293–310.

Vitasse, Y., Delzon, S., Dufrêne, E., Pontailler, J.Y., Louvet, J.M., Kremer, A., & Michalet, R. (2009). Leaf phenology sensitivity to temperature in European trees: Do within-species populations exhibit similar responses? *Agricultural and Forest Meteorology*, *149*(5), 735–744.

Zhang, Z.Z., Zhao, P., McCarthy, H.R., Zhao, X.H., Niu, J.F., Zhu, L.W., Ni, G.Y., Ouyang, L., & Huang, Y.Q. (2016). Influence of the decoupling degree on the estimation of canopy stomatal conductance for two broadleaf tree species. *Agricultural and Forest Meteorology*, *221*, 230–241.